

Augmentation of active wing-bending control with a supplementary adaptive feed-forward control algorithm

Andreas Wildschek, Rudolf Maier*, Ravindra Jategaonkar**, and Horst Baier****

**EADS Innovation Works Germany, Structures Engineering, Production & Mechatronics, Munich, 81663, Germany*

***Deutsches Zentrum für Luft- und Raumfahrt, Institut für Flugsystemtechnik, Braunschweig, 38108, Germany*

****Technical University of Munich, Lehrstuhl fuer Leichtbau, Garching, 85747, Germany*

Abstract

Large transport aircraft are commonly equipped with robust feedback controllers for wing-bending alleviation. As shown in this paper by numeric simulations, the performance of such a feedback system can be dramatically increased by an augmentation with an adaptive feed-forward controller. The most important constraint for proper feed-forward wing-bending control is sufficient coherence between the reference signal (obtained through the alpha probe) and the vibration excitation of the aircraft. Flight test results are presented in order to emphasize that this constraint is fulfilled. Thus it is concluded that the combination of robust feedback with adaptive feed-forward control is a powerful approach for very efficient alleviation of wing-bending vibrations.

1. Introduction

Wing-bending vibration excited by turbulence and manoeuvres causes high dynamic loads and reduces handling qualities and flight comfort especially for large transport aircraft. Thus these aircraft are commonly equipped with robust feedback controllers since the 1970s¹. HAHN & KOENIG² also successfully reduced the vibrational wing loads of the DLR Advanced Technologies Testing Aircraft (ATTAS) research aircraft with a feedback system and additionally reduced static gust loads with an additive feed-forward controller. Feed-forward control appeared to be very effective to reduce gust loads. A modified alpha probe signal provided a proper reference signal for feed-forward control. Moreover in WILDSCHKE ET AL³ it was shown, that turbulence induced wing-bending vibrations may be addressed much more effectively by feed-forward than by feedback control if an according reference signal is available in the frequency range of the wing-bending mode. An adaptive algorithm (based on a finite impulse response (FIR) controller) was used to realize maximum performance and robust stability at the same time. However such a feed-forward controller cannot be used to alleviate wing-bending vibrations excited by manoeuvres.

By supplementing state-of-the-art feedback wing-bending control systems with an additional adaptive feed-forward controller the control performance can be maximized and dynamic loads excited by turbulence and manoeuvres can be addressed at the same time. Moreover, the latest investigations show, that by the use of an adaptive infinite impulse response (IIR) controller the number of adaptive coefficients can be significantly decreased compared to the FIR controller, thus reducing the computational effort. However, robust stability is much more difficult to prove for an adaptive IIR controller than for an adaptive FIR controller. Proper conditions for robust stability of an adaptive feed-forward wing-bending control system based on an FIR controller are already available³. For the adaptive IIR wing-bending control system robust stability still has to be investigated. Due to the changing fuel load conditions, an aircraft structure represents a time varying plant. The proposed adaptation of the feed-forward path prevents from a performance degradation due to time variations in the plant, and due to the eventual presence of modelling errors³.

In order to test the performance of an adaptive IIR wing-bending control system, numerical simulation were performed with a state space model of the longitudinal dynamics of a 4 engine example transport aircraft. The

turbulence excitation was modelled as an angle of attack variation constantly distributed over the wingspan. This variation was generated by von Kármán filtered white noise. Symmetrically driven ailerons served as actuators for wing-bending control. Regardless an FIR or an IIR controller is used, augmenting feedback wing-bending control with adaptive feed-forward control would very effectively help to reduce fatigue of the wing roots of big transport aircraft and thus offers a great chance to reduce the structural weight of the wing box.

2. Augmentation of robust feedback with adaptive feed-forward wing-bending control

In order to provide maximum possible performance of wing-bending control, and alleviate turbulence- and pilot-induced wing-bending vibrations, the inner robust feedback loop (generally used for wing-bending control) is augmented by an adaptive feed-forward path, see Figure 1.

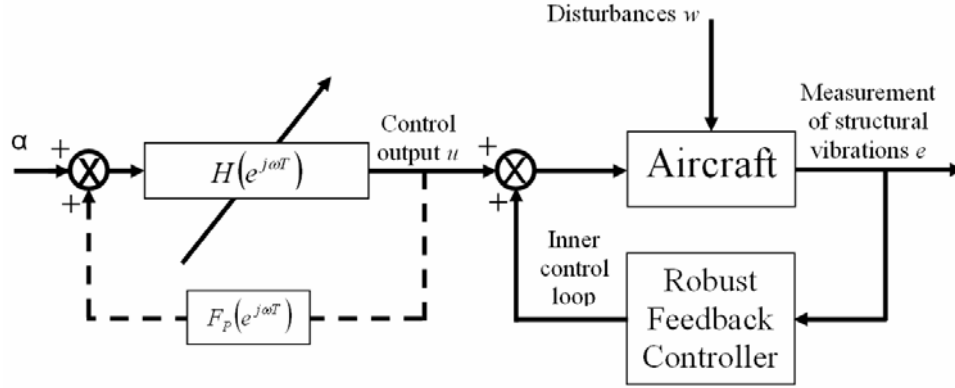


Figure 1: Combination of robust feedback and adaptive feed-forward wing-bending control.

The feed-forward path uses the dynamic share of the alpha probe signal as reference signal for the adaptive feed-forward controller $H(e^{j\omega T})$. The control output u of the feed-forward controller is then added to the control output of the inner feedback control loop. Note that it is assumed that the parasitic feedback $F_p(e^{j\omega T})$ from the feed-forward control output u to the alpha probe signal is small enough to be neglected, and that any significant influence of rigid body motions on the reference signal α is compensated, as proposed in HAHN & KOENIG². It is further assumed that the influence of structural vibrations on the alpha probe measurement is small enough to be neglected. Disturbances w (i.e. turbulence, gust, pilot commands) excite wing-bending vibrations. The wing-bending vibrations are measured by a modal acceleration sensor, or error sensor, compare Figure 2. As proposed in JEANNEAU ET AL.⁶, the vertical accelerations of the two wings Nz_{LW}, Nz_{RW} are added and the vertical acceleration of the centre of gravity Nz_{CG} is subtracted from half of this value, see Eq. (1). This approach allows for observation of vertical wing-bending, but inhibits measurement of rigid body motions.

$$e = \left[\frac{(Nz_{LW} + Nz_{RW})}{2} - Nz_{CG} \right] \quad (1)$$

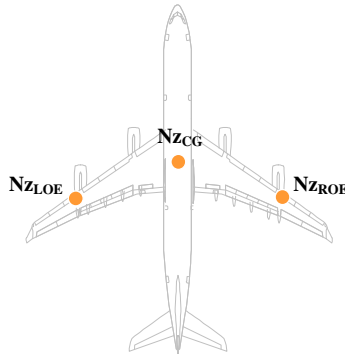


Figure 2: Modal acceleration sensor.

Thus both, the robust feedback controller and the adaptive feed-forward controller aim at the minimization of the error signal e . For the robust feedback path a band pass H_∞ controller was used, that would only damp the wing-bending mode without influencing any other modes, compare JEANNEAU ET AL.⁶. The additional adaptive feed-forward control path seeks at the minimisation of the H_2 -norm of the error signal in the frequency range between 0.5 and 4 Hz (i.e. frequency range of the first significant structural modes). The feed-forward controller $H(e^{j\omega T})$, which minimizes the H_2 -norm of the error signal is⁵:

$$H_{opt}(e^{j\omega T}) = -\frac{S_{rd}(e^{j\omega T})}{S_{rr}(e^{j\omega T})} \quad (2)$$

Thereby $S_{rd}(e^{j\omega T})$ denotes the cross power spectrum between the filtered reference signal r and the desired signal d . The filtered reference signal r is the reference probe signal α filtered by the transfer function $G(e^{j\omega T})$. The transfer function $G(e^{j\omega T})$ is the control path from the control output u to the error sensor signal e , thus including the inner control loop, compare Figure 1. The desired signal d is the effect of disturbances w on the error signal, ω is the angular frequency, and T is the sampling period. $S_{rr}(e^{j\omega T})$ is the power spectral density of the filtered reference signal r .

$$S_{rd}(e^{j\omega T}) = G^*(e^{j\omega T}) S_{ad}(e^{j\omega T}) \quad (3)$$

$$S_{ad}(e^{j\omega T}) = \langle DFT(\alpha)^*(e^{j\omega T}) D(e^{j\omega T}) \rangle \quad (4)$$

$$S_{rr}(e^{j\omega T}) = \langle R^*(e^{j\omega T}) R(e^{j\omega T}) \rangle \quad (5)$$

With D , and R denoting the Discrete Fourier Transforms (DFTs) of the desired signal d , and the filtered reference signal r . $S_{ad}(e^{j\omega T})$ denotes the cross power spectrum between the reference probe signal α and the desired signal d . The brackets $\langle \dots \rangle$ denote the expectation value, and $*$ means complex conjugation. For the realization of the adaptive feed-forward controller mainly two approaches deem appropriate, use of an FIR feed-forward controller, or use of an IIR feed-forward controller. With the complex variable z , the discrete transfer functions denote:

FIR controller:
$$H(z) = h_0(n) + h_1(n)z^{-1} + h_2(n)z^{-2} + \dots + h_{N-1}(n)z^{-N+1} \quad (6)$$

IIR controller:
$$H(z) = \frac{A(z)}{B(z)} = \frac{a_0(n) + a_1(n)z^{-1} + a_2(n)z^{-2} + \dots + a_I(n)z^{-I}}{1 + b_1(n)z^{-1} + b_2(n)z^{-2} + \dots + b_J(n)z^{-J}} \text{ with } I \leq J \quad (7)$$

Thereby n denotes the time step, N is the filter length of the FIR controller, and I and J are the numbers of zeros, and poles of the IIR controller. IIR controllers have the advantage that an infinite impulse response can be represented with a finite number of controller coefficients (i.e. $I+J+2$). Thus usually a low number of IIR controller coefficients is sufficient. However, the FIR controller has the advantage that it cannot converge to an unstable controller since only the zeros are adapted and all poles remain in the origin. The high robust stability of adaptive FIR control is shown in WILDSCHKE ET AL.³, where an adaptive feed-forward wing-bending control system based on an FIR controller is presented including a detailed stability analysis.

An algorithm for feed-forward IIR controller adaptation that offers promising convergence behaviour is the so-called filtered-U algorithm developed by ERIKSSON⁴. The time domain adaptation law for the filtered-U algorithm is:

$$a_i(n+1) = a_i(n) - c_1 \cdot e(n)r(n-i) \quad (8)$$

$$b_j(n+1) = b_j(n) - c_2 \cdot e(n)\tilde{u}(n-j) \quad (9)$$

Thereby $r(n-i)$ is the n -ith sample of the reference signal α filtered by the transfer function $\hat{G}(e^{j\omega T})/B(e^{j\omega T})$, and $\tilde{u}(n-j)$ is the n -jth sample of the IIR controller's output u filtered by a transfer function $\hat{G}(e^{j\omega T})/B(e^{j\omega T})$. As an

approximation the factor $1/B(e^{j\omega T})$ may be removed for simplification of the adaptation algorithm^{4,7}. In both cases the controller converges to almost the same IIR approximation of $H_{opt}(e^{j\omega T})$, compare Figure 4, green and blue line. The transfer function $\hat{G}(e^{j\omega T})$ is an estimate of the control path from IIR control output u to the error sensor signal e . This means that $\hat{G}(e^{j\omega T})$ also includes the inner robust feedback loop. In WANG & REN⁷ constraints on the accuracy of the estimate $\hat{G}(e^{j\omega T})$ for stable convergence of the IIR adaptation are provided. The choice of the convergence coefficients c_1 and c_2 determine the convergence speed of the adaptive IIR controller towards the optimum $H_{opt}(e^{j\omega T})$, and thus also the stability of the adaptation. Due to the lack of theoretic stability boundaries for c_1 and c_2 , the convergence coefficients were chosen empirically. By the use of an adaptive IIR controller the number of required controller coefficients can be significantly reduced compared to the FIR approach, see Figure 3. After 7500 samples adaptation starting from $a_j(n=1)=b_i(n=1)=0$ a 2nd order IIR controller provides more than 90% reduction of the cost function (i.e. H₂-norm of the error signal) for the example aircraft, which is almost the same as for a 3rd order, but much less than for a 1st order IIR controller. Note that for the results of this paper only IIR controllers with same number of poles and zeros were considered for convenience. Figure 4 shows the transfer functions of 2nd order IIR controllers with $\hat{G}(e^{j\omega T})/B(e^{j\omega T})$ and with $\hat{G}(e^{j\omega T})$ filtering of the reference signal, as well as the transfer function of a 64th order FIR wing-bending controller after 7500 samples convergence time.

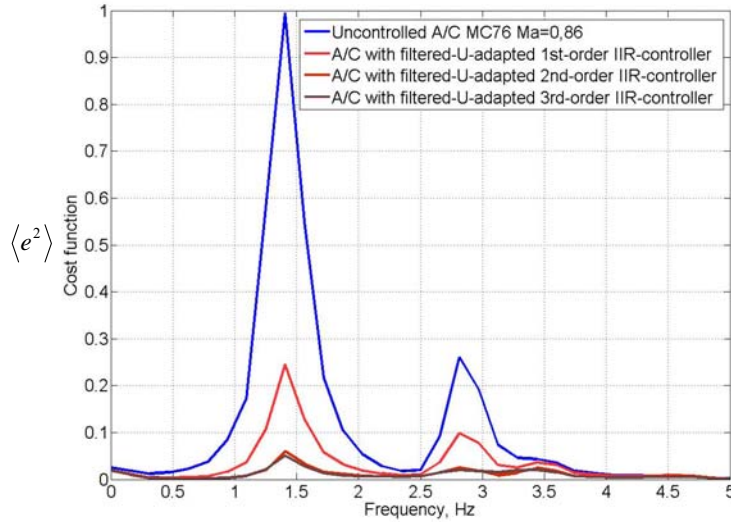


Figure 3: Performance with IIR feed-forward controllers of different orders after 7500 samples.

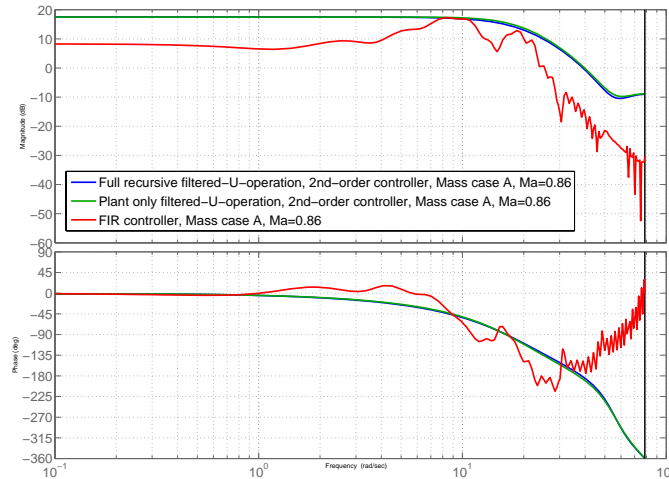


Figure 4: 2nd order IIR controllers with $\hat{G}(e^{j\omega T})/B(e^{j\omega T})$ and $\hat{G}(e^{j\omega T})$ filtered α signal; 64th order FIR controller

3. Constraints for proper feed-forward wing-bending control

Feed-forward control of structural vibrations is possible only when an appropriate reference signal is available⁵. Moreover the performance of the proposed feed-forward wing-bending control system depends mainly on the coherence between the reference signal α (i.e. modified alpha probe signal), and the share of the error signal coming from the atmospheric turbulence excited aircraft, also called desired signal d , see Eq. (10).

$$\frac{\mathcal{E}_{\min}(e^{j\omega T})}{S_{dd}(e^{j\omega T})} = 1 - \frac{|S_{rd}(e^{j\omega T})|^2}{S_{rr}(e^{j\omega T})S_{dd}(e^{j\omega T})} = 1 - \frac{|S_{ad}(e^{j\omega T})|^2}{S_{aa}(e^{j\omega T})S_{dd}(e^{j\omega T})} = 1 - \gamma_{ad}^2(e^{j\omega T}) \quad (10)$$

The term $\gamma_{ad}^2(e^{j\omega T})$ is defined as the (quadratic) coherence function between the reference probe signal α and the desired signal d . Thereby $S_{aa}(e^{j\omega T})$ is the power spectral density of the reference probe signal, and \mathcal{E}_{\min} is the minimum control error:

$$\mathcal{E}_{\min} = S_{dd}(e^{j\omega T}) + S_{rd}^*(e^{j\omega T})H_{opt}(e^{j\omega T}) \quad (11)$$

Thus we see that the higher the coherence function between α and the desired signal d , the smaller the remaining control error. For the theoretic value of $\gamma_{ad}^2(e^{j\omega T}) = 1$ the minimum control error is zero, which means that the wing-bending vibration could then be erased completely through feed-forward control.

In order to obtain a realistic numeric value of the coherence function $\gamma_{ad}^2(e^{j\omega T})$, flight test data from the DLR Advanced Technologies Testing Aircraft (ATTAS), compare HAHN & KOENIG², was evaluated. For this coherence analysis data from a flight in turbulent atmosphere without any significant pilot inputs was used. The first structural Eigen mode of the test aircraft is a symmetric pylon-bending mode at about 3.5 Hz, compare Figure 5. The first symmetric vertical wing-bending mode has an Eigen frequency $\omega_{\text{wing-bending}}$ of about 5 Hz.

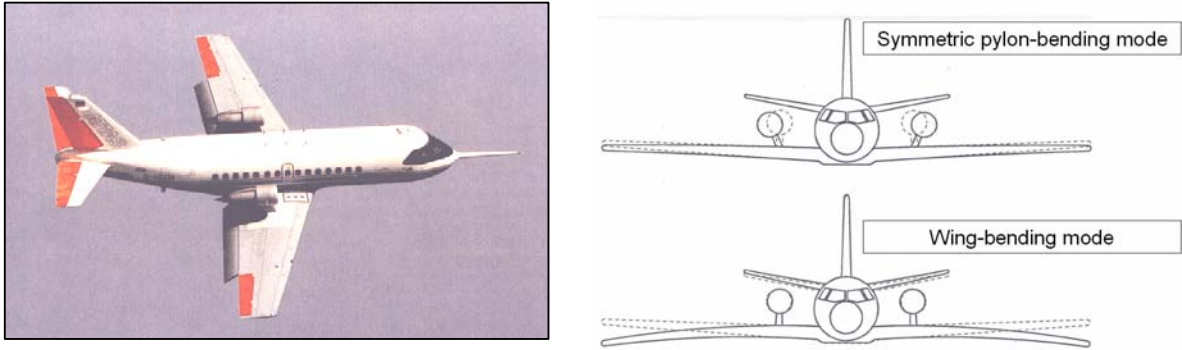


Figure 5: Eigen modes of the ATTAS research aircraft

These modes can be observed very accurately by a *lateral* acceleration sensor mounted at the engine location (unfortunately no proper modal acceleration sensor signal as described in Eq. (1) was available). This *lateral* acceleration sensor does not measure any disturbing longitudinal rigid body motions which is very advantageous for the coherence analysis since the rigid body motions then do not have to be compensated in the acceleration signal. Figure 6 shows the coherence function between said lateral acceleration sensor signal and the ATTAS's nose boom alpha vane (blue line) and the coherence function between said lateral acceleration sensor signal and the alpha vane mounted at the front fuselage (red line). We see that the nose boom alpha vane and the alpha vane mounted at the front fuselage show about the same coherence with the lateral engine acceleration signal at the frequencies of the Eigen modes. This is in favour of the *frozen field assumption*. However at frequencies where no structural modes

exist, the coherence is very low because there is hardly any acceleration signal. This has no effect on feed-forward vibration control because there is nothing to control at these frequencies.

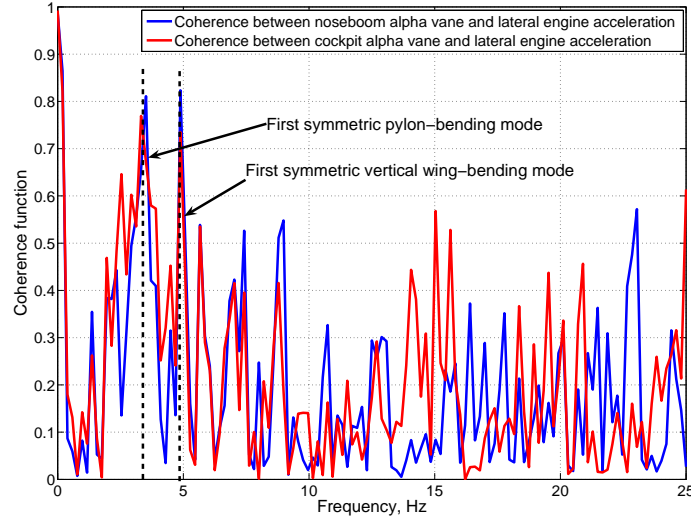


Figure 6: Coherence functions from an ATTAS test flight in severe turbulence.

In the frequency range of Eigen modes of the ATTAS (i.e. 3.5 Hz and 5 Hz) the coherence function $\gamma_{ad}^2(e^{j\omega})$ is better than 75% which (according to Eq. 10) is sufficient for 50% reduction of accelerations by feed-forward control only, i.e.

$$\left[\frac{\varepsilon_{\min}(e^{j\omega_{\text{wing-bending}}T})}{S_{dd}(e^{j\omega_{\text{wing-bending}}T})} \right]^{1/2} \approx 0.5 \quad (12)$$

Note that thereby it is assumed that hardly any of the shown coherence is due to a structural coupling between the alpha probes and the lateral engine acceleration sensor, at least in the frequency range of structural modes that shall be controlled. This still needs to be proven.

4. Numeric simulation of feed-forward augmented wing-bending control

Numeric simulations were performed with a state space model of the longitudinal dynamics of a 4 engine example transport aircraft. An alpha probe modelled at aircraft's front fuselage was used as reference sensor. The output of the alpha probe is denoted α_{air} .

$$\alpha_{air} = \alpha_{wind} + \alpha_{ground} \quad (13)$$

α_{air} is composed of two parts, namely α_{wind} which is generated by von Kármán filtered white noise, and represents atmospheric turbulence, and α_{ground} which is an output of the state space model representing the movement of the alpha probe's mounting node due to aircraft motions and structural vibrations (α_{ground} also contains parasitic feedback, which was small enough to be neglected for the example aircraft). For feed-forward wing-bending control α_{wind} is required. Thus any significant α_{ground} has to be compensated in the alpha probe output, such as proposed in HAHN & KOENIG². Furthermore the alpha probe output is high pass filtered to acquaint the dynamic share required as reference for feed-forward wing-bending control, compare Figure 7. The turbulence excitation w of the aircraft was modelled as span-wise constant angle of attack variation α_w .

$$\alpha_w = (\alpha_{wind} + \alpha_v) \cdot z^{-\delta} \quad (14)$$

Thereby an angle of attack α_v is added to the angle of attack coming from the turbulent atmosphere α_{wind} in order to represent the coherence degradation between reference measurement and turbulence exiting the wing. The time-lag between mounting node of the alpha probe and aerodynamic centre of the wing is generated by a time delay $z^{-\delta}$. In order to achieve a 75% coherence between reference measurement α_{air} and aircraft excitation α_w , α_v must be von Kármán filtered white noise with $(1/3)^{1/2}$ magnitude of α_{wind} , but with different initial seed. This follows from Eq. (10).

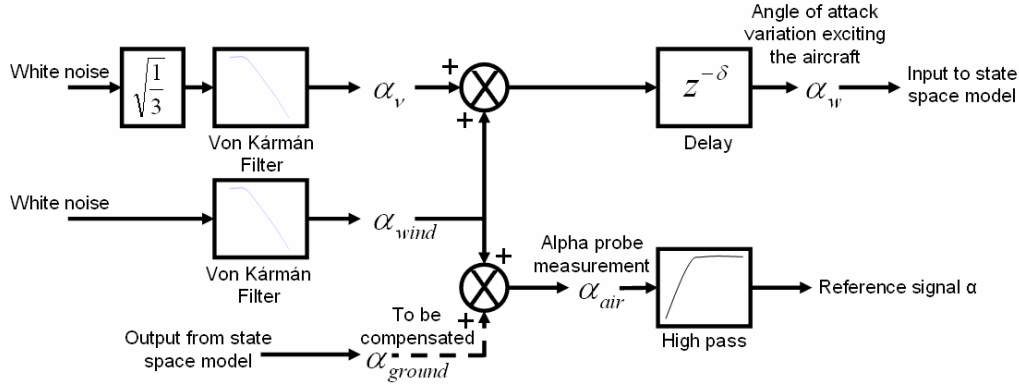


Figure 7: Modelling of turbulence excitation and turbulence measurement with 75% coherence

Finally Figure 8 illustrates the mean magnitude of the error sensor output e against the frequency for the 4 engine example aircraft. The blue line denotes the uncontrolled aircraft, and the red line is the mean magnitude of the error sensor output for robust feedback control with a band pass controller. The violet and the green line illustrate the mean magnitude of the error sensor output for robust feedback control with adaptive feed-forward augmentation using an FIR, and using an IIR controller. The coherence between the reference signal α and the desired signal d is modelled to be 75% in the simulations.

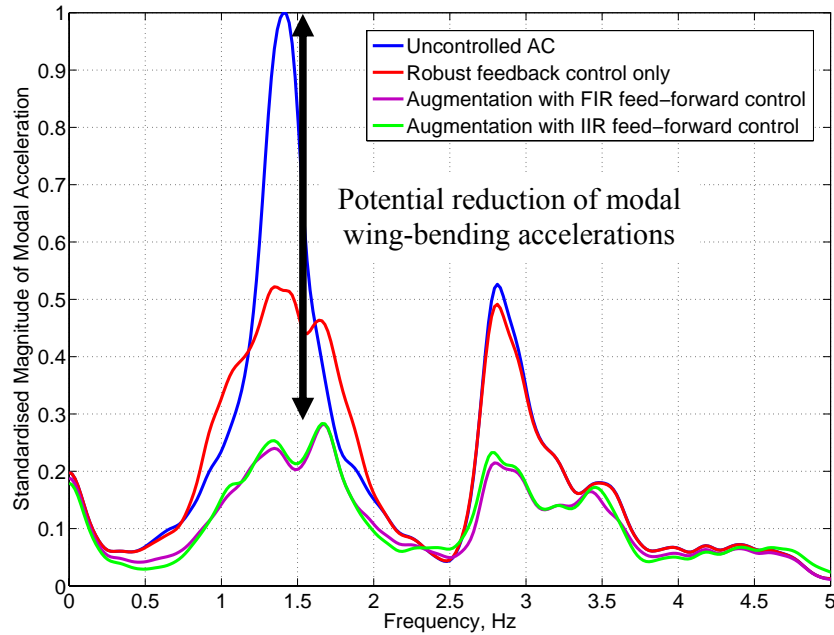


Figure 8: Performance of different control approaches

The augmentation of robust feedback wing-bending control increases the vibration attenuation depending on the coherence. As predicted from Eq. (10), feed-forward control alone reduces modal wing-bending accelerations by about 50% for a 75% coherence between α and d , regardless an FIR or an IIR controller is used. In combination with a feedback controller that almost doubles the wing-bending damping compared to the uncontrolled aircraft, more than 70% reduction of wing-bending acceleration magnitude was achieved in the numerical simulations.

5. Conclusions

Augmentation of existing robust feedback wing-bending controllers with an adaptive feed-forward path is proposed for improved vibration alleviation. A modified alpha probe signal is used as reference for feed-forward control. Through flight test data it is shown that such a reference sensor would be sufficient for 50% reduction of the modal acceleration magnitude by the feed-forward controller alone. In combination with feedback control more than 70% vibration reduction were achieved in numerical simulations with a state space model of the longitudinal dynamics of a 4 engine transport aircraft.

Thereby two approaches have been investigated, namely FIR and IIR feed-forward control. The performance of the two approaches is about the same. The IIR approach has the advantage that less controller coefficients are required than for the FIR approach, thus saving computing costs. Regardless an FIR or an IIR controller is used, augmenting feedback wing-bending control with feed-forward control would very effectively help to reduce fatigue of the wing roots of big transport aircraft and thus offers a great chance to reduce the structural weight of the wing box.

For the FIR adaptation a robust stability proof is already available. Thus the FIR approach seems to have a great chance to be certified for line operation. Thereby the big advantage of the proposed adaptation of the feed-forward path is, that the FIR controller would converge to the optimum even in the presence of modelling errors and would track the optimum for a time-varying plant. However, the problem of robust stability is not yet solved for the IIR approach. Thus, the IIR feed-forward augmentation might not be ready to be certified for line operation, but can be used as an online design tool on flight tests. For the adaptation only an estimate of the control path from the control output to the error sensor signal is required, which can be easily online identified at the beginning of the flight test. The adapted IIR controller could then be implemented as robust feed-forward controller for line operation.

References

- [1] JOHNSTON, J. F., ET AL. Accelerated Development and Flight Evaluation of Active Controls Concepts for Subsonic Transport Aircraft Volume 1 – Load Alleviation/Extended Span Development and Flight Test. NASA CR-159097, pages 2-11, 1979.
- [2] HAHN, K.-U. KOENIG, R. ATTAS flight test and simulation results of the advanced gust management system LARS. In *AIAA Atmospheric Flight Mechanics Conference*, Hilton Head Island, SC, Aug 10-12, 1992.
- [3] WILDSCHKE, A., MAIER, R., HOFFMANN, F., JEANNEAU, M., AND BAIER, H. Active Wing Load Alleviation with an Adaptive Feed-forward Control Algorithm. In *AIAA Guidance, Navigation, and Control Conference and Exhibit*, Keystone, Colorado, 21.-24. August, 2006.
- [4] ERIKSSON, L. Development of the filtered-U algorithm for active noise control. *Journal of the Acoustical Society of America*, Volume 89, pages 257-265, 1991.
- [5] ELLIOTT, S. J. Signal Processing for Active Control, Academic Press, London, 2001.
- [6] JEANNEAU, M., AVERSA, N., DELANNOY, S., HOCKENHULL, M. Awiator's study of a Wing Load Control: Design and Flight-test Results. *16th IFAC Symposium on Automatic Control in Aerospace*, St. Petersburg (RUSSIA), 14-18 June 2004.
- [7] WANG, K., REN, W. Convergence analysis of the filtered-U algorithm for active noise control. *Journal of Signal Processing*, Volume 73, pages 255-266, 1999.



This page has been purposely left blank